Developmental Biology **224,** 299–311 (2000)
doi:10.1006/dbio.2000.9798, available online at http://www.idealibrary.com on IDEAL®

Disruption of Gastrulation and Heparan Sulfate Biosynthesis in EXT1-Deficient Mice

Xin Lin,*[,1] Ge Wei,† Zhengzheng Shi,‡ Laurence Dryer,* Jeffrey D. Esko,† Dan E. Wells,*[,2] and Martin M. Matzuk‡[,§,¶]

**Department of Biology and Biochemistry, University of Houston, Houston, Texas 77204; †Glycobiology Research & Training Center, Department of Cellular and Molecular Medicine, University of California at San Diego, La Jolla, California 92093-0687; and ‡Department of Pathology, §Department of Cell Biology, and ¶Department of Molecular and Human Genetics, Baylor College of Medicine, Houston, Texas 77030*

Mutations in the EXT1 gene are responsible for human hereditary multiple exostosis type 1. The *Drosophila* EXT1 homologue, *tout-velu,* regulates Hedgehog diffusion and signaling, which play an important role in tissue patterning during both invertebrate and vertebrate development. The EXT1 protein is also required for the biosynthesis of heparan sulfate glycosaminoglycans that bind Hedgehog. In this study, we generated EXT1-deficient mice by gene targeting. EXT1 homozygous mutants fail to gastrulate and generally lack organized mesoderm and extraembryonic tissues, resulting in smaller embryos compared to normal littermates. RT-PCR analysis of markers for visceral endoderm and mesoderm development indicates the delayed and abnormal development of both of these tissues. Immunohistochemical staining revealed a visceral endoderm pattern of Indian hedgehog (Ihh) in wild-type E6.5 embryos. However, in both EXT1-deficient embryos and wild-type embryos treated with heparitinase I, Ihh failed to associate with the cells. The effect of the EXT1 deletion on heparan sulfate formation was tested by HPLC and cellular glycosyltransferase activity assays. Heparan sulfate synthesis was abolished in EXT1 −/− ES cells and decreased to less than 50% in +/− cell lines. These results indicate that EXT1 is essential for both gastrulation and heparan sulfate biosynthesis in early embryonic development.

Key Words: **EXT1; gene targeting; embryonic development; heparan sulfate biosynthesis.**

INTRODUCTION

Hereditary multiple exostoses (EXT) is a skeletal disorder that primarily affects endochondral bone growth (Wicklund *et al.,* 1995). It is characterized by the formation of cartilage-capped exostoses and short stature. EXT shows an autosomal dominant inheritance and is ascribed to mutations at three distinct genetic loci. The EXT1 locus, at 8q24.1 (Ahn *et al.,* 1995), and the EXT2 locus, at 11p11–12 (Stickens *et al.,* 1996), have been cloned and define a novel multigene family that has potential tumor suppressor function.

EXT1 is a conserved protein, demonstrating 99% identity between mouse and human homologues (Lin and Wells, 1997; Wei *et al.,* 2000). Recent studies have demonstrated that both EXT1 and EXT2 are associated with glycosyltransferase activities required for the biosynthesis of heparan sulfate (Lind *et al.,* 1998; McCormick *et al.,* 1998, 2000; Toyoda *et al.,* 2000; Wei *et al.,* 2000). EXT1 and EXT2 appear to form a heterodimer *in vivo* which is required for maximal transferase activities and this complex may represent the biologically relevant form of the enzymes (McCormick *et al.,* 2000).

Cell surface heparan sulfate is known to function in receiving signaling molecules. Studies have shown that the *Drosophila* homologue of EXT1 (*tout-velu*) is specifically required for the diffusion of Hedgehog signaling (Bellaiche *et al.,* 1998; The *et al.,* 1999). Hedgehog precursor proteins undergo an internal autoproteolytic cleavage that generates a 19-kDa cholesterol-linked N-terminal peptide and a C-terminal peptide of 26–28 kDa (Lee *et al.,* 1992, 1994).

[1] Present address: Howard Hughes Medical Institute, UCSF Box 0703, San Francisco, CA 94143.

[2] To whom correspondence should be addressed. Fax: (713) 743-2636. E-mail: dwells@uh.edu.

0012-1606/00 $35.00

Through its cholesterol moiety, the N-terminal peptide associates with the cell surface while the C-terminal peptide is freely diffusible (Lee *et al.*, 1994). The N-terminal peptide is both necessary and sufficient for short- and long-range Hedgehog signaling in *Drosophila* and in vertebrates (Lee *et al.*, 1994; Porter, 1995). Since the N-terminal Hedgehog peptide remains tightly associated with the surface of the cells producing it, it is unclear how long-range signaling is achieved. The recently identified role of *tout-velu* suggests that membrane-targeted Hh movement requires *tout-velu*-synthesized heparan sulfate (Bellaiche *et al.*, 1998; The *et al.*, 1999). A mammalian homologue of Hedgehog, Indian hedgehog (Ihh), has a well-documented role in regulating the rate of chondrocyte differentiation and bone development (Vortkamp *et al.*, 1996; Zou *et al.*, 1997). Ihh is also known to be involved in mediating differentiation of extraembryonic endoderm during early mouse embryogenesis (Becker *et al.*, 1997). If EXT1 functions similarly in both mammals and *Drosophila*, the etiology of EXT may relate to abnormalities in Ihh diffusion due to a failure in synthesis of specific cell surface glycosaminoglycans (GAGs), which leads to defective signaling.

To investigate the role of EXT1 in mammals and provide a system to study EXT1 function *in vivo*, we disrupted the EXT1 gene by homologous recombination in mouse ES cells. In contrast to humans, in which EXT is an autosomal dominant disorder, mice heterozygous for the targeted EXT1 mutation do not show exostoses. Homozygous null mice die by embryonic day 8.5 due to defects in mesoderm formation and failure of extraembryonic egg cylinder elongation. In addition, heparan sulfate synthesis is disrupted in EXT1 mutants, indicating that EXT1 encodes an essential component of the glycosyltransferase complex required for heparan sulfate assembly.

MATERIALS AND METHODS

Gene Targeting

A 9-kb 129/SvEv mouse genomic clone containing 5′ UTR, exon 1, and part of intron 1 of the mouse EXT1 gene was isolated. To target the EXT1 gene in murine embryonic stem (ES) cells, a positive–negative selection strategy was used. A targeting vector was generated by cloning the 5′ and 3′ regions (0.9-kb *Bgl*II–*Sca*I and 2.2-kb *Sal*I–*Eco*RI fragments, respectively, of the 9-kb genomic clone) into plasmid pLGII (obtained from Dr. Lin Gan, unpublished data), which contains PGK-*neo* and MC1-*tk* cassettes separated by multiple cloning sites (Fig. 1A). A 0.3-kb fragment, including part of both exon 1 and intron 1, was deleted and a promoterless LacZ marker gene with a 3′ translation stop codon was placed downstream of and in frame with the exon 1 sequences (Fig. 1A). The targeting vector (pXL-EXT1) was linearized at a unique *Not*I site and electroporated into the 129SvEv-derived AB2.1 ES cells. Southern blot hybridization confirmed that 18% of the ES cell clones were targeted correctly. Two independent clones (EXT1-85-A3 and EXT1-85-A6) were injected into blastocysts as described (Matzuk *et al.*, 1992). Chimeric males obtained following blastocyst injection were bred with C57/B16 females. Both independent ES cell clones demonstrated germ-line transmission, and the mutant phenotypes generated using both clones were identical. The targeted mutation has been maintained in both 129SvEv/C57/B16 hybrid and 129/SvEv inbred backgrounds. The phenotypes of the EXT1 mutant embryos are similar for both genetic backgrounds.

Genotype Analysis

Genotypes were determined by genomic Southern blot analysis or by PCR (Figs. 1B and 1C). Genomic DNA from ES cells and mice was isolated as described (Matzuk *et al.*, 1992). To determine genotype by Southern blot analysis, DNA was digested with *Eco*RI and hybridized with a 5′ probe (Fig. 1B). Embryos analyzed at E6.5, E7.5, and E8.5 were genotyped by PCR (Fig. 1C). Staging of embryos was performed as is standard (i.e., E0.5 is 1 PM on the day of the copulation plug). PCR amplification for genotyping was performed using the following primers: forward EXT1 primer 5′-gttaccaaaacattctagcggc-3′, reverse EXT1 primer 5′-cggtgttgtctctgtcacagcg-3′, and the targeting vector primer 5′-cttctttttgcttcctccg-3′, which distinguished wild-type (400 bp) from mutant (300 bp) alleles.

Morphological, Histological, and in Situ Hybridization Analyses

E6.5, E7.5, and E8.5 embryos from timed matings of heterozygotes were either isolated intact in their deciduae or dissected out and analyzed morphologically. Intact embryos were fixed overnight in 4% paraformaldehyde at 4°C, dehydrated, and embedded in paraffin. Sections (8 μm thick) were cut and stained with hematoxylin and eosin or were processed for *in situ* hybridization. The probes used for *in situ* hybridization included EXT1 (Lin *et al.*, 1997), Brachyury (Herrmann, 1991), and H19 (Poirier *et al.*, 1991). Probes were labeled with [^{35}S]UTP and *in situ* hybridization was performed as described (Wilkinson *et al.*, 1993).

Generation and Differentiation of ES Cell Lines

ES cell lines were generated using blastocysts collected from heterozygote matings as previously described (Evans *et al.*, 1981). Briefly, blastocysts were isolated and cultured on fibroblast feeder cell layers (SNL76/7) for 4–7 days. Blastocyst outgrowth colonies were then trypsinized and grown on new feeder cell layers. Southern blot analysis was performed to identify the genotype of these ES cell lines (Fig. 1D). For differentiation into embryoid bodies, ES cells were lightly trypsinized and then transferred to bacterial dishes without fibroblast feeder cell layers (Robertson, 1987).

RNA and Immunohistochemical Analyses

The expression patterns of various genes in the wild-type and mutant embryoid bodies were compared by semiquantitative RT-PCR analysis. Total RNA (1 μg) was reverse transcribed using a cDNA synthesis kit for RT-PCR (Boehringer Mannheim). For all genes analyzed, 2 μl (1/10) of the cDNA reaction was used for PCR amplification. The PCR amplification of the cDNA remained linear after 30 cycles (data not shown). The PCR products were separated on a 2% agarose gel and Southern blot analyses were performed by use of radioactive end-labeled internal primers as probes. Primers used for PCR amplification and internal probing are listed in Table 1.

For immunohistochemical staining, deparaffined sections of

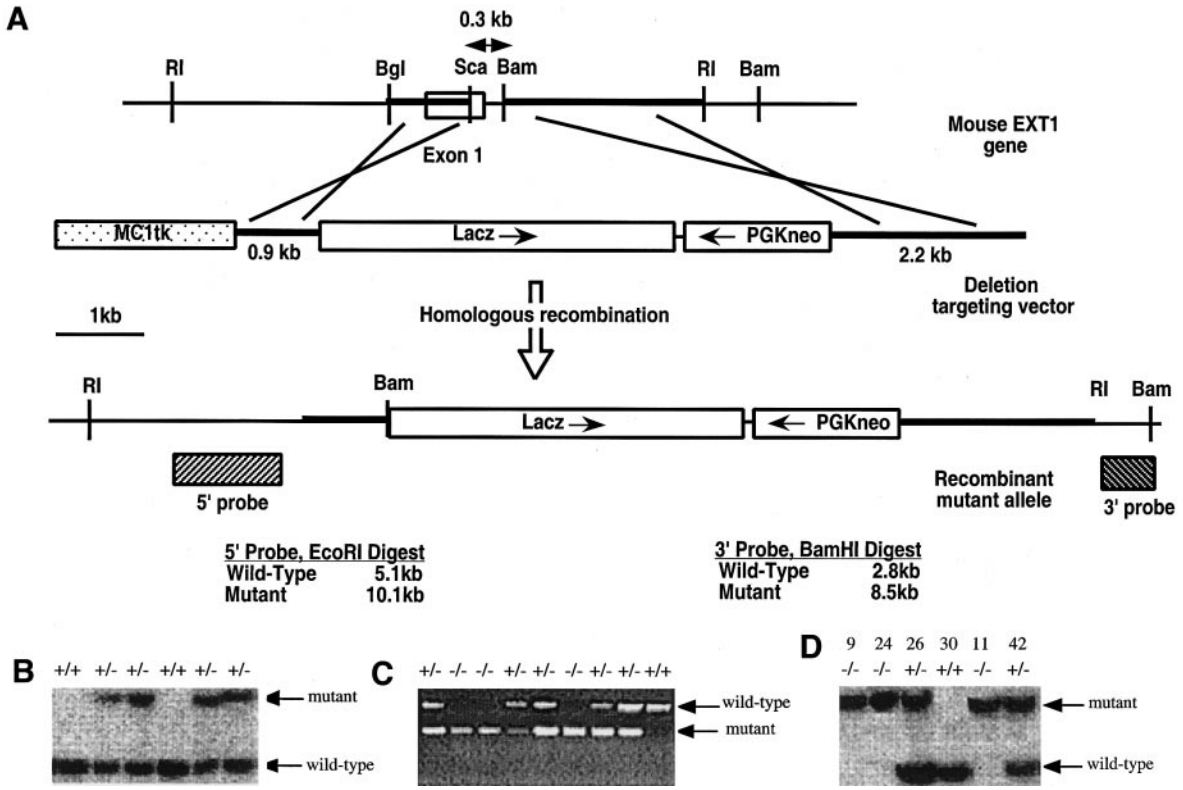

FIG. 1. Gene targeting at the EXT1 locus. (A) Disruption of EXT1 through homologous recombination in ES cells. Maps of the wild-type EXT1 locus (top), the targeting vector (middle), and the predicted targeted locus after homologous recombination (bottom). The targeting vector deletes part of exon 1 and intron 1. PGK-*neo* and MC1-*tk* expression cassettes are shown. Lacz indicates a promoterless LacZ marker gene. Recombinants were detected by Southern blot analysis using 5′ and 3′ probes and *Eco*RI (RI) and *Bam*HI (Bam), respectively, as diagnostic enzymes. (B) Southern blot analysis of genomic DNA isolated from postnatal mice generated from intercrosses of EXT1 +/− mice. No EXT −/− newborn mice were recovered. (C) PCR analysis of E6.5–E8.5 embryos demonstrating the recovery of wild type (+/+), heterozygous (+/−), and homozygous (−/−) mutant embryos. (D) Southern blot analysis of ES cell clones derived from blastocyst cultures and hybridized with the 5′ external probe. RI, *Eco*RI; Bgl, *Bgl*II; Sca, *Sca*I; Bam, *Bam*HI.

E6.5 embryos were incubated with 5E1 monoclonal antibody (myeloma cells obtained from the Development Studies Hybridoma Bank, University of Iowa) directed against the N-peptide of Sonic hedgehog, which is known to cross-react with Indian hedgehog (Ericson *et al.*, 1996; Grabel *et al.*, 1997). Staining was detected with a Histomouse-SP kit (Zymed Laboratories, Inc., South San Francisco) using a biotinylated secondary antibody. Prior to incubation with the 5E1 antibody, wild-type E6.5 sections were overlaid with 2.5 mU of heparitinase I (Sigma, St. Louis, MO) in 0.5 ml of buffer (100 mM sodium chloride, 1 mM calcium chloride, 50 mM sodium Hepes, pH 7.0, containing 25 μg of BSA) or with buffer only, for 2 h at 37°C. After being rinsed with 0.5% casein (w/v) in PBS, sections were incubated with 5E1 antibody; the staining was then detected with the Histomouse-SP kit.

Analyses for Glycosaminoglycan Chains and Cellular Enzyme Activities

ES cells cultured for 48 h were radiolabeled with 50 μCi/ml of $^{35}SO_4$ (Dupont NEN) in sulfate-deficient growth medium (Esko *et al.*, 1986). [^{35}S]GAG chains were isolated by DEAE chromatography and a sample was treated with chondroitinase ABC at 37°C overnight (Bame *et al.*, 1989). Treated and untreated chains were separated by anion-exchange HPLC. Glycosaminoglycans were eluted with a linear gradient of NaCl (0.2–1 M) using a flow rate of 1 ml/min and by increasing the NaCl concentration by 10 mM/min. The effluent from the column was monitored for radioactivity with an in-line radioactivity detector (Radiomatic Flow One/β; Packard Instruments) with sampling rates every 6 s and data averaged over 1-min intervals.

GlcNAc transferase and GlcA transferase activities were assayed using oligosaccharide acceptors prepared from the capsular polysaccharide of *Escherichia coli* K5 as described (Lidholt *et al.*, 1992). Embryoid bodies were differentiated and collected in homogenization buffer (0.25 M sucrose, 20 mM Tris–Cl, pH 7.4, 1 mM phenylmethylsulfonyl fluoride, 1 μg/ml each leupeptin and pepstatin A) and sonicated. Each 25-μl reaction for GlcNAc transferase contained 25 mM Mops, pH 6.5, 20 mM $MnCl_2$, 0.3% Triton X-100 (w/v), 1 mM UDP-[6-^{3}H]GlcNAc (220 Ci/mol), 25 μg cleaved *N*-acetylheparosan, and 10–20 μg of cell homogenate protein. To

TABLE 1
Primers Used for PCR Amplification and Internal Probing

Primer	Sequences: F, forward; R, reverse; I, internal		T_m°C
EXT1	(F) 5′-tccctggaggattgttcgtc-3′	(R) 5′-tagcagctcctgtcaacac-3′	55
	(I) 5′-gccaaatcccagtactgtgcgcag-3′		
T	(F) 5′-tgctgcctgtgagtcataac-3′	(R) 5′-accaggtgctatattgcc-3′	54
	(I) 5′-gctgggagctcagttctttcgaggc-3′		
BMP2	(F) 5′-tgcttcttagacggactgcggt-3′	(R) 5′-ggaacgtgcgcacggtgttggc-3′	56
	(I) 5′-ggccgggacccgctgtcttctag-3′		
BMP4	(F) 5′-cctcttcaacctcagcagcatcc-3′	(R) 5′-cacacccctctaccaccatctcc-3′	59
	(I) 5′-caccagggccagcatgtcagaatcagc-3′		
GATA1	(F) 5′-ggccccttgtgaggccagagag-3′	(R) 5′-tccagccagattcgacccccgc-3′	60
	(I) 5′-gtatgcaatgcctgcggcctcta-3′		
HNF1	(F) 5′-ttctaagctgagccagctgcagacg-3′	(R) 5′-gctgaggttctccggctctttcaga-3′	62
	(I) 5′-tgacacggatgacgatggggaagac-3′		
GATA4	(F) 5′-cagccctacccagcctacat-3′	(R) 5′-gtgccccagccttttactttg-3′	56
	(I) 5′-aaaccagaaaacggaagcccaagaacc-3′		
AFP	(F) 5′-atactcaagaactcaccccaacct-3′	(R) 5′-ctcacaccaaagcgtcaacacatt-3′	56
	(I) 5′-tgagacaggaaggttggggtgag-3′		
TRANSF	(F) 5′-acctcctactacgctgtggctgtg-3′	(R) 5′-gggttctttccttcggtgttatcc-3′	60
	(I) 5′-actgttcagctctcctcttgg-3′		
HPRT	(F) 5′-gctggtgaaaaggacctctcgaagtg-3′	(R) 5′-atggccacaggactagaacacctgc-3′	55
	(I) 5′-caaagcctaagatgagcgcaagttg-3′		

assay GlcA transferase, each 25-μl reaction contained 25 mM Mes, pH 5.5, 20 mM $MnCl_2$, 0.03% Triton X-100 (w/v), 2 mM UDP-[1-^{3}H]GlcA (250 Ci/mol), 70 μg β-glucuronidase-treated cleaved *N*-acetylheparosan, and 10–20 μg of cell homogenate protein. Reactions were terminated after 1 h by boiling, and the products were isolated by DEAE–Sephacel chromatography, mixed with chondroitin sulfate carrier (1 mg), precipitated in 80% ethanol, and quantified by liquid scintillation spectrometry.

RESULTS

EXT1 Is Expressed during Early Embryogenesis

We have previously determined that EXT1 mRNA first begins to accumulate between E5.5 and E6.5 during mouse embryogenesis and EXT1 transcripts can be detected in all tissues examined in adult mice (Lin *et al.*, 1998). *In situ* hybridization analysis of E6.5 and E7.5 wild-type embryos also revealed a widespread tissue distribution. A strong signal was apparent in the ectoplacental cone, the ectoderm, the parietal and visceral endoderm, and the trophoblastic giant cells (Figs. 2A and 2B). At E6.5, EXT1 expression was absent in the extraembryonic portion of the ectoderm (Fig. 2A). However, in E7.5 embryos EXT1 expression extended into the entire egg cylinder (Fig. 2B). The ubiquitous expression pattern of EXT1 at all stages suggests it has an essential role during mammalian development.

Targeted Disruption of EXT1 Results in Embryonic Lethality

To create an EXT1 loss-of-function mutation, we generated a targeted mutation via homologous recombination in mouse ES cells (Fig. 1A). Two independent mutant ES clones heterozygous for the EXT1 mutation were expanded for injection into C57/Bl6 blastocysts. Both clones gave rise to chimeric mice that were mated with C57/Bl6 females to obtain germ-line transmission of the mutant alleles. Chimeras from both clones transmitted the mutation through the germ line, and about 50% of the offspring with agouti coat color (22/48) were heterozygous as determined by Southern blot analysis. Mice heterozygous for the EXT1 mutation were phenotypically normal. Thirty heterozygous mice from two different genetic backgrounds (C57/B16/129/SvEv hybrid and 129/SvEv inbred) were followed for a period of up to 14 months. No exostoses or increase in tumor incidence was observed in these mice compared with wild-type controls. EXT1 heterozygotes were intercrossed to generate EXT1 −/− mutants, and their genotypes were determined by Southern blot analysis (Fig. 1B). No homozygotes were found among 168 mice genotyped postnatally, suggesting that the homozygous null mutation is embryonically lethal (Table 2). To determine the timing of this lethality, embryos from EXT1 +/− matings were genotyped by Southern blot analysis or PCR (Figs. 1B and 1C). No EXT1 −/− embryos were identified after embryonic day E8.5 (Table 2).

EXT1 Mutant Embryos Fail to Form Mesoderm and Show Defects in Egg Cylinder Elongation

To determine the defects that cause the embryonic lethality in the absence of EXT1, E6.5–E8.5 embryos were analyzed both morphologically and histologically. Wild-type E6.5 embryos have an extended extraembryonic region

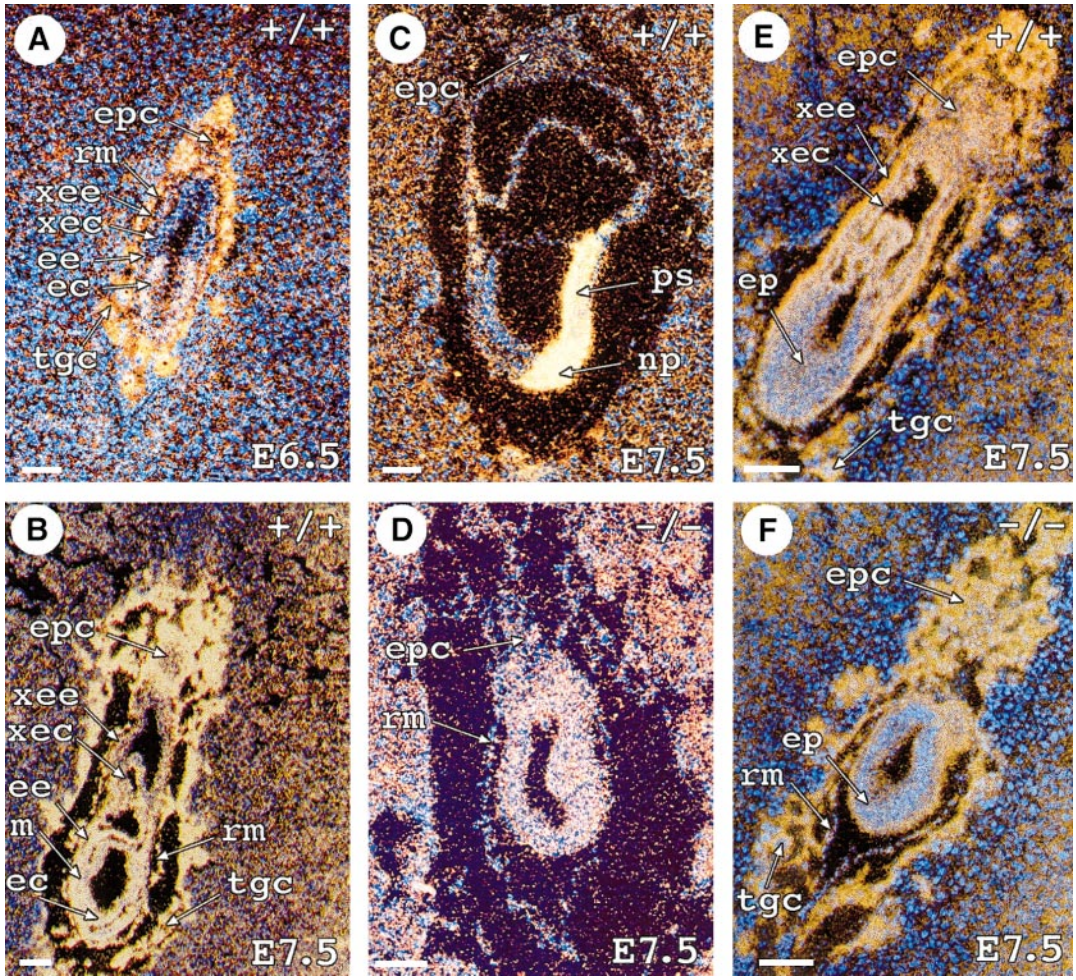

FIG. 2. Distribution of EXT1, Brachyury (T), and H19 by *in situ* hybridization analysis. Sagittal sections of (A) E6.5 embryo probed with EXT1, (B) E7.5 embryo probed with EXT1, (C) E7.5 wild-type embryo probed with T, (D) E7.5 EXT1 −/− embryo probed with T, (E) E7.5 wild-type embryo probed with H19, and (F) E7.5 EXT1 −/− embryo probed with H19. All images are dark-field views of probes overlaid on the DAPI images. epc, ectoplacental cone; xee, extraembryonic endoderm; xec, extraembryonic ectoderm; rm, Reichert's membrane; ee, embryonic endoderm; ec, embryonic ectoderm; tgc, trophoblast giant cell; ps, primitive streak; np, notochord plate; ep, epiblast; m, mesoderm. Scale bars: (A–F) 200 μm.

and distinct extraembryonic/embryonic boundary. In contrast E6.5 EXT1 −/− embryos failed to develop an extraembryonic region and were much smaller than their littermate controls (Fig. 3A). However, the ectoplacental clones of the EXT1 mutant embryos appeared to be normal. In wild-type embryos, a clear morphological distinction is apparent between the embryonic and the extraembryonic tissues (especially the endodermal cells). Embryonic endoderm cells have a largely squamous morphology, whereas extraembryonic endoderm cells have a characteristic columnar shape, apical vacuoles, and a microvillous "brush" border (Fig. 3D). Mutant E6.5 EXT1 −/− embryos were completely lacking of this characteristic extraembryonic structure, and the ectoplacental cone was attached to the embryonic portion of the embryos. In addition, the embry-

TABLE 2

Genotype Analyses of Offspring from EXT1 Heterozygote Matings

	Normal		Abnormal		
	+/+[a]	+/−[a]	−/−[a]	Resorbed[b]	Total
E6.5	12 (28%)	20 (48%)	7 (17%)	3 (7%)	42
E7.5	10 (23%)	23 (52%)	9 (20%)	2 (5%)	44
E8.5	11 (27%)	17 (41%)	5 (12%)	8 (20%)	41
E9.5	6 (25%)	14 (58%)	0 (0%)	4 (17%)	24
Newborn	62 (37%)	106 (63%)	0 (0%)		168

Note. The percentages of the different genotypes appear in parentheses.

[a] The genotype was determined by Southern blot or PCR analysis as described under Materials and Methods.

[b] Resorbed embryos were not genotyped.

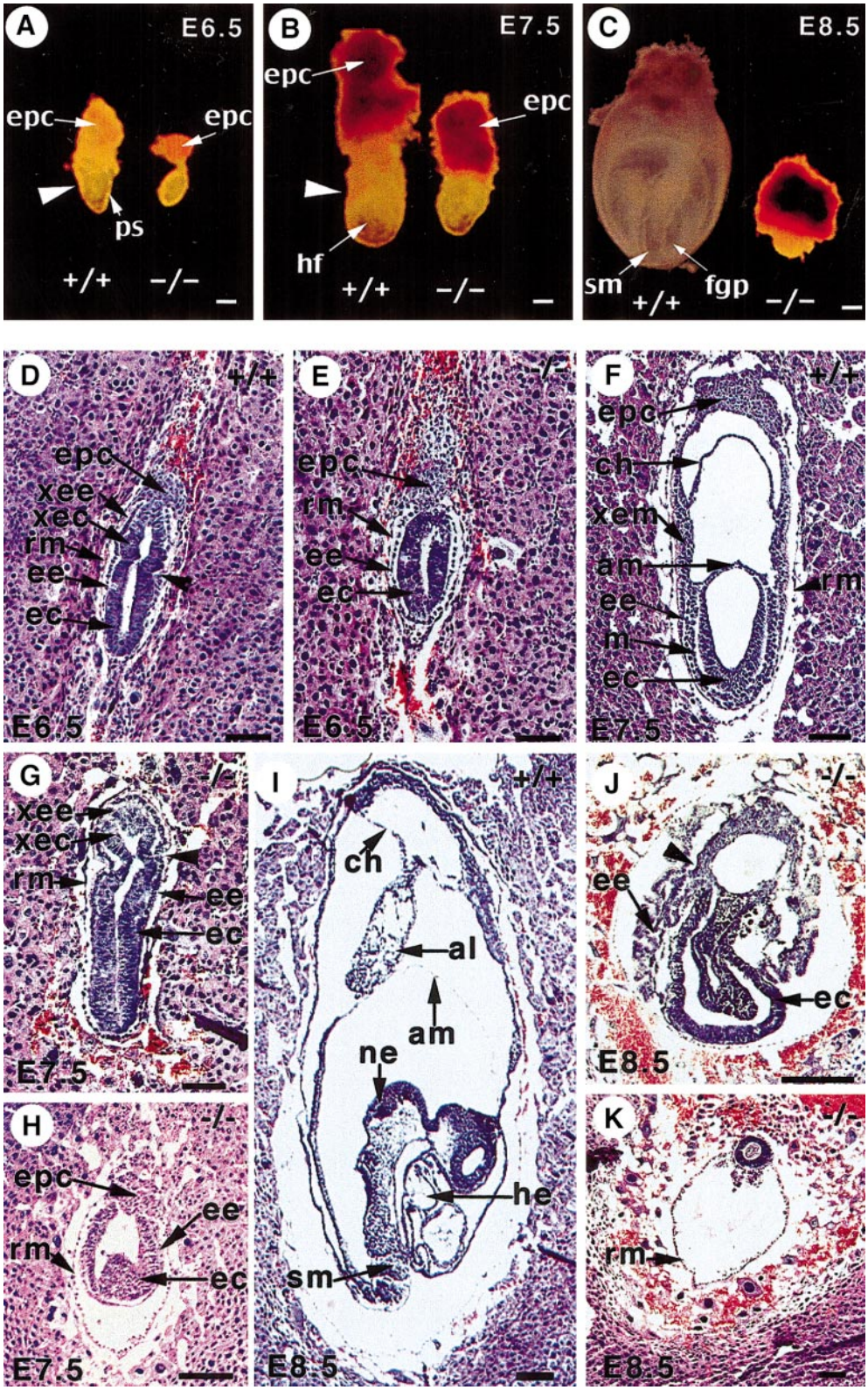

onic region of the EXT1 −/− embryos was underdeveloped compared to normal embryos (Fig. 3E).

By E7.5, wild-type embryos demonstrated a primitive streak and obvious headfold (Fig. 3B). However, no such structures could be identified in EXT1 −/− embryos. By E7.5, the chorion and amnion in the extraembryonic region of wild-type embryos were evident, and embryos were divided into the ectoplacental cavity, the exocoelomic cavity, and the amniotic cavity. In addition, mesoderm generated at the primitive streak had spread through the embryo (Fig. 3F). Although E7.5 EXT1 −/− mutant embryos increased in size compared to stage E6.5, they were still much smaller than wild-type littermates (Fig. 3B). EXT1 −/− mutant embryos at E7.5 remained as two-layered cylinders of ectoderm and endoderm, with no mesoderm and with no obvious extraembryonic tissue (Figs. 3G and 3H). In addition, the embryonic cavity remained as the proamniotic canal and the amnion and chorion were absent (Figs. 3G and 3H). At E8.5, normal embryos had developed a notochord, a few somites, a foregut pocket, and a primitive heart (Fig. 3I). By this stage, the majority (~80%) of the homozygous embryos were resorbed. In the surviving embryos, the tissues were poorly organized and failed to resemble their wild-type counterparts (Figs. 3C, 3J, and 3K).

As a follow-up on these histological studies, *in situ* hybridization analysis was performed on early embryos using Brachyury (an early mesodermal marker) and H19 (a marker for extraembryonic tissue development). Brachyury is first detected in premesodermal cells of the primitive ectoderm at the onset of gastrulation around E6.5 (Kispert *et al.*, 1993). In wild-type E6.5 embryos, intense labeling of a small cluster of cells was detected in the primitive streak (data not shown), while in wild-type E7.5 embryos, such intense labeling was detected over the entire streak and notochordal plate (Fig. 2C). However, in EXT1 −/− embryos at E6.5 (data not shown) and E7.5 (Fig. 2D), no Brachyury expression was detected. This confirmed the histological analysis indicating that no primitive streak or mesoderm forms in EXT1 −/− embryos.

H19 is activated in extraembryonic cell types at the time of implantation (Poirier *et al.*, 1991). Its expression marks the extraembryonic endoderm and ectoderm, the ectoplacental cone, and the trophoblastic giant cells, but not the epiblast (Fig. 2E). H19 expression in the mutants was detected only in the ectoplacental cone, the trophoblastic giant cells, and the visceral endoderm. No other portion of the egg cylinder was labeled (Fig. 2F). This confirmed that there were no organized extraembryonic tissues in the EXT1-deficient egg cylinder.

Mutant Embryoid Bodies Show Altered Differentiation

ES cells derived from *in vitro* blastocyst cultures will differentiate into embryoid bodies (EBs) when cultured in suspension. This process resembles the formation of the developing conceptus at the egg-cylinder stage (Doetschman *et al.*, 1985). To characterize the function of EXT1 during early embryonic development, ES cell lines, derived from control (+/+, +/−) or EXT1 −/− blastocysts, were isolated. Genotype analysis confirmed that EXT1 −/− cell lines could be identified (Fig. 1D). Morphologically, the EXT1-deficient ES cell lines resembled the control ES cell lines (data not shown). We next examined the effect of absence of EXT1 on embryoid body formation. By day 12, more than 60% of the wild-type ES cells formed cystic EBs with large fluid-filled cavities. In contrast, the EXT1 homozygous mutant EBs failed to form such cavities (Fig. 4A). A well-defined and characteristic visceral yolk-sac endoderm layer extended around the wild-type EBs, whereas a poorly differentiated primitive endoderm structure covered the homozygous mutant EBs (Fig. 4B). To define the expression patterns of the *in vitro* differentiated mutant ES cells, specific markers were examined by semiquantitative RT-PCR at different time points during the differentiation process. Brachyury (T) (Keller *et al.*, 1993), BMP2 (Winnier *et al.*, 1995), BMP4 (Winnier *et al.*, 1995), and Gata-1 (Elefanty *et al.*, 1997) are markers for mesoderm differentiation. HNF1 (Roach *et al.*, 1994), α-fetoprotein (AFP) (Dziadek, 1979), Transferrin (Doetschman *et al.*, 1985), and Gata-4 (Keller *et al.*, 1993) are markers for endoderm differentiation. EXT1 was expressed throughout the differentiation of wild-type EBs (Fig. 4C). In contrast to *in vivo* observations, Brachyury expression was comparable

FIG. 3. Morphological and histological analyses of wild-type and EXT1 −/− mutant embryos. (A–C) Morphology of dissected embryos. (A) E6.5 +/+ embryo (left) and EXT1 −/− mutant littermate (right); large arrowhead indicates the boundary between extraembryonic and embryonic regions of the wild-type embryo. (B) E7.5 wild-type embryo (left) at the headfold stage and EXT1 mutant littermate (right), which is underdeveloped with no headfold structure and extraembryonic tissues. (C) E8.5 wild-type embryo (left), demonstrating a foregut invagination and obvious somites, and an EXT1 mutant littermate (right). (D–I) Hematoxylin–eosin staining of sagittal sections of embryos within intact decidual tissues at E6.5 (D, E), E7.5 (F, G, H), and E8.5 (I, J, K). E6.5 EXT1 −/− mutant embryo (E) lacks extraembryonic tissues, and the ectoplacental cone is adjacent to the embryonic tissue. E7.5 EXT1 mutant embryos (G, H) lack mesoderm and fail to demonstrate proper elongation of the egg cylinder, and the extraembryonic portions are either small (G) or absent (H). Wild-type E8.5 embryo (I) shows structures such as chorion, heart, neural ectoderm, and somites. Two EXT1 mutant littermates (J, K) lack these structures. epc, ectoplacental cone; ps, primitive streak, hf, headfold; fgp, foregut pocket; sm, somites; xee, extraembryonic endoderm, xec, extraembryonic ectoderm; rm, Reichert's membrane; ch, chorion; xem, extraembryonic mesoderm; am, amnion; m, mesoderm; al, allantois; ne, neural ectoderm, he, heart. Large arrowhead points to the extraembryonic and embryonic boundary. Scale bars: 200 μm.

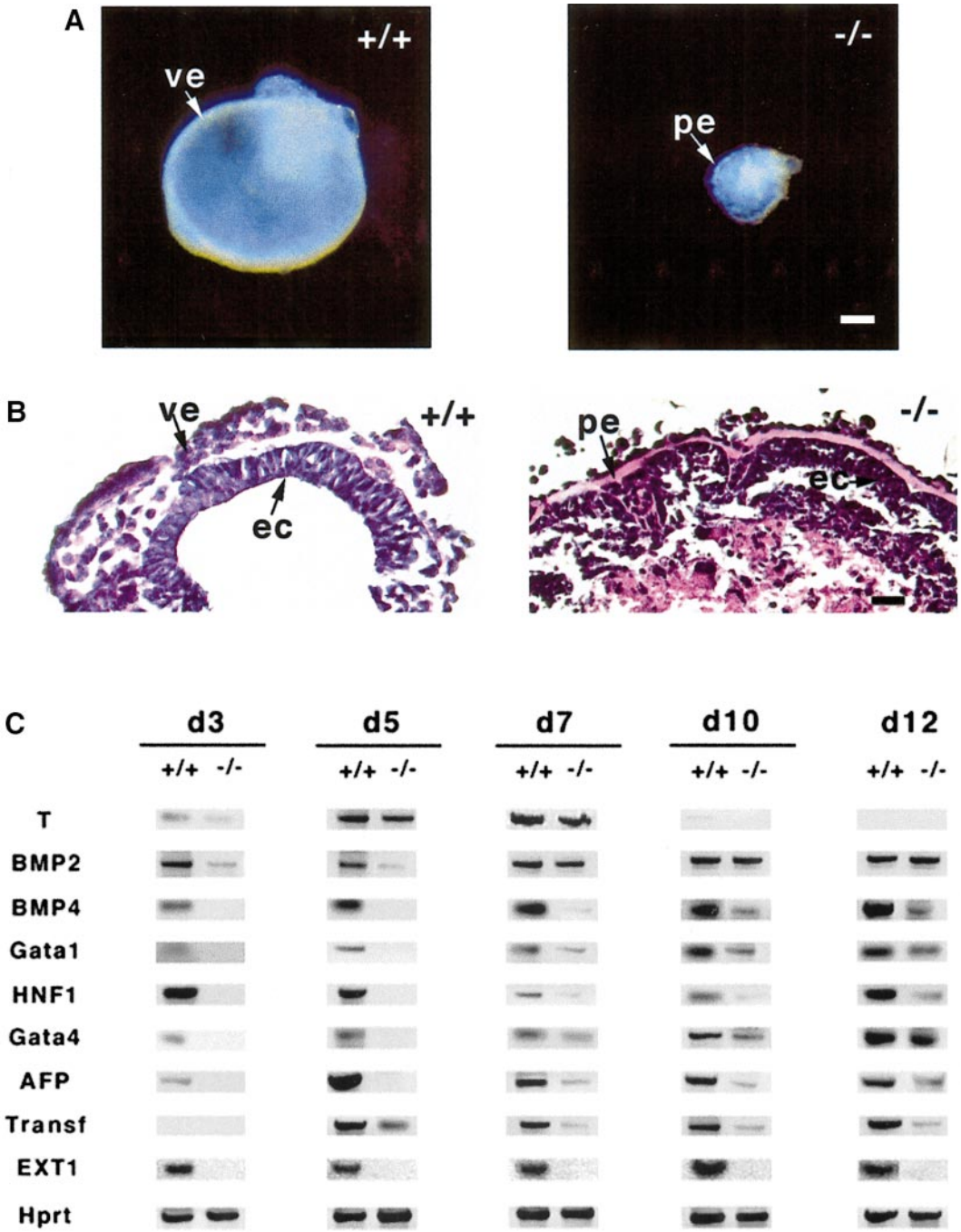

FIG. 4. Altered *in vitro* differentiation in EXT1 −/− ES cells. (A) Two representative day 10 EBs. A wild-type EB (left) forms a large cystic cavity and an EXT1 −/− ES cell-derived EB (right) is smaller and does not develop a cavity. (B) Paraffin sections (8 μm) of day 10 EBs were stained with H&E. The wild-type (left) has a defined visceral endoderm layer, whereas the EXT1 −/− mutant (right) has a poorly differentiated endoderm layer which resembles primitive endoderm. (C) Semiquantitative RT-PCR analysis of differentiation markers of endodermal and mesodermal lineage. RNA was extracted from wild-type and EXT1 −/− EBs at day 3, 5, 7, 10, and 12 of *in vitro* culture. Expressions of Brachyury (T), Gata-1, BMP2, and BMP4 were examined as mesodermal markers; HNF1 and Gata-4 as early endodermal markers, and AFP and Transferrin as late endodermal markers. ve, visceral endoderm; pe, primitive endoderm; Transf, Transferrin. Scale bars: (A) 200 μm, (B) 100 μm.

in normal and homozygous mutant EBs (Fig. 4C). Gata-1 expression of homozygous mutant EBs was virtually absent at early time points (days 3 and 5 of cultures), but was comparable to wild type by day 12 of culture (Fig. 4C), suggesting a delay in hematopoietic mesoderm differentiation. BMP2 is normally expressed first in the extraembryonic mesoderm associated with the proamniotic canal and later in the amnion and chorion (Winnier *et al.*, 1995; Zhang *et al.*, 1996), while BMP4 is expressed in the posterior primitive streak and extraembryonic mesoderm (Winnier *et al.*, 1995). BMP2 and BMP4 are also downstream targets of Hedgehog signaling in vertebrate systems (Laufer *et al.*, 1994; Roberts *et al.*, 1995). In EXT1-deficient EBs, BMP2 expression was low at days 3 and 5 of culture but was comparable to wild type after day 7. However, BMP4 expression was absent at days 3 and 5 culture and remained at very low levels through day 12 in EXT1 homozygous EBs. In contrast, BMP4 expression was upregulated during normal EB differentiation (Grabel *et al.*, 1998). HNF1 and Gata-4 are normally expressed early in the specification of visceral endoderm (Roach *et al.*, 1994; Soudais *et al.*, 1995), whereas AFP and Transferrin are late markers for visceral endoderm differentiation (Dziadek, 1979; Doetschman *et al.*, 1985). HNF1 expression was greatly decreased at all time points in homozygous mutant EBs (Fig. 4C). Gata-4 expression was absent at days 3 and 5 culture in EXT1 −/− EBs and remained low after day 7 (Fig. 4C). In EXT1 −/− clones, AFP was absent completely at early time points and gradually increased at later stages (days 10 and 12). This is in contrast to the high level of expression at day 5 in wild-type clones (Fig. 4C). Transferrin expression was detected in wild-type and homozygous mutant EBs at day 5, but unlike wild-type clones, its expression remained at a low level at later stages in EXT1 −/− clones (Fig. 4C). These defects in expression markers for mesoderm and endoderm differentiation suggest an impairment of these lineages in early development of EXT1 −/− EBs.

The Absence of EXT1 Affects Hedgehog Association with the Cell Surface

Tout-velu, the *Drosophila* homologue of the EXT1 gene, is required for Hedgehog diffusion and signaling in *Drosophila* (Bellaiche *et al.*, 1998; The *et al.*, 1999). Indian hedgehog is the only Hedgehog protein expressed during gastrulation in mammals and an important regulator of developmental processes (Grabel *et al.*, 1998; Bueno *et al.*, 1996; Becker *et al.*, 1997; Bitgood and McMahon, 1995; Vortkamp *et al.*, 1996; St-Jacques *et al.*, 1999). To investigate the connection between heparan sulfate synthesis and Hedgehog signaling, immunohistochemical staining with 5E1 monoclonal antibody against Ihh-N was carried out in sections of E6.5 embryos, and results from wild-type and EXT1 −/− mutants were compared. In wild-type E6.5 sections (Figs. 5A and 5B), a strong staining was observed around the surface of visceral endoderm cells. After digestion with heparitinase I, this staining was significantly

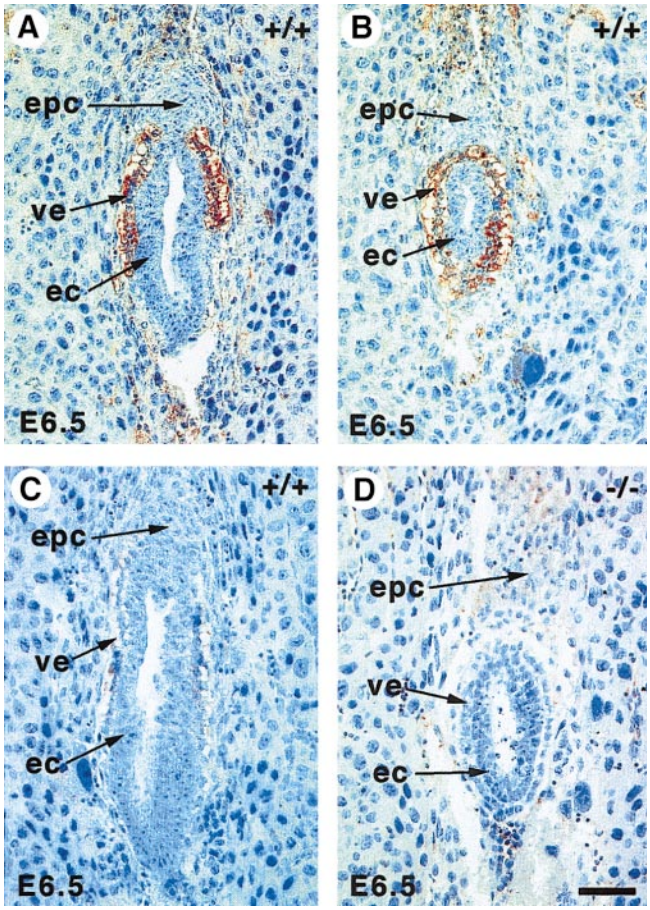

FIG. 5. Immunohistochemical analysis of Indian hedgehog N-terminal peptide expression in E6.5 wild-type untreated (A, B), E6.5 wild-type digested with heparitinase I (C), and EXT1 −/− (D) embryo sections. Indian hedgehog N-terminal peptide was detected in visceral endoderm layer of E6.5 wild-type embryo (A, B), the staining was significantly reduced in the heparitinase I-treated E6.5 wild-type embryo (C), and no staining was detected in EXT1 −/− E6.5 embryo sections (D). ec, ectoderm; epc, ectoplacental cone. Scale bar: 200 μm.

reduced in the wild-type E6.5 embryo sections (Fig. 5C). No specific staining was observed in EXT1 −/− E6.5 embryo sections (Fig. 5D). This is despite that fact that Ihh protein and mRNA are expressed in E6.5 EXT1 −/− embryos at levels similar to those of wild-type embryos, as assayed by Western blotting and RT-PCR (data not shown). Hence, EXT1-synthesized cell surface heparan sulfate appears to be important for the association of Ihh-N with the cell surface.

Defects of Heparan Sulfate Formation in EXT1 Mutants

Studies have suggested that EXT1 encodes a subunit of the copolymerase that catalyzes the formation of heparan

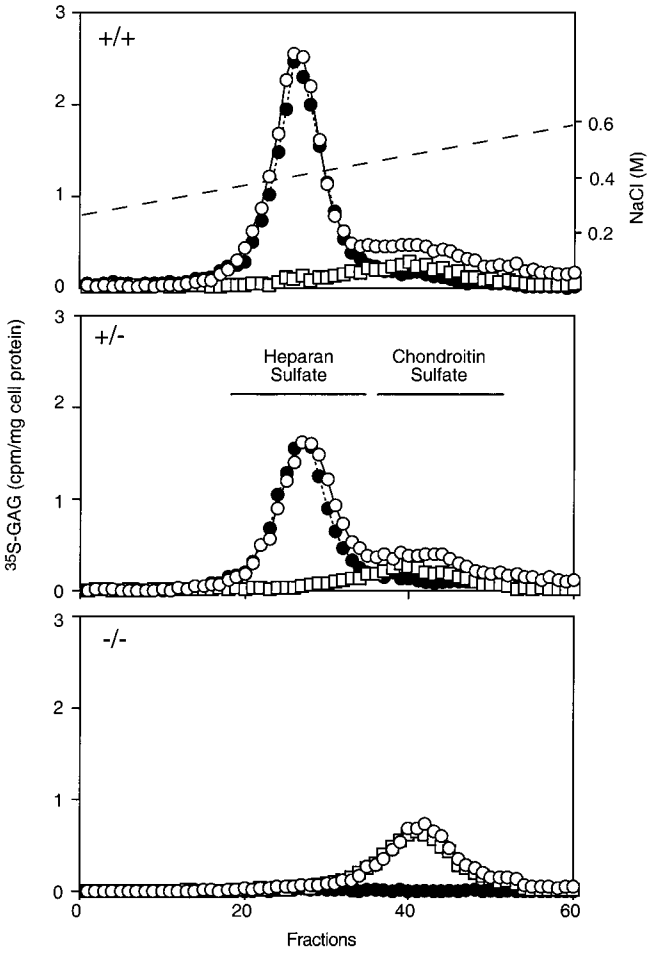

FIG. 6. Embryoid bodies were incubated in medium containing $^{35}SO_4$ in order to radiolabel the glycosaminoglycan chains to constant radiospecific activity. Samples were analyzed by anion-exchange HPLC before and after treatment with chondroitinase ABC or nitrous acid (Bame and Esko, 1989) using a gradient of NaCl for elution. The positions of the heparan sulfate and chondroitin sulfate are indicated by the solid bars and were determined by enzymatic or chemical degradation of the chains. Open circles, untreated samples. Open squares, after treatment with nitrous acid. Filled circles, after chondroitinase ABC treatment.

sulfate (McCormick *et al.*, 1998). To determine if ablation of the mouse EXT1 altered heparan sulfate formation, ES cells derived from wild-type, heterozygous, and homozygous null mice were cultured with $^{35}SO_4$ to radiolabel the polysaccharide chains. As shown in Fig. 6, wild-type ES cells make mostly heparan sulfate. Similar results were obtained when the cells were radiolabeled with [6-^{3}H]glucosamine (data not shown). ES cells also produce a small amount of chondroitin sulfate/dermatan sulfate that elutes at a higher salt concentration and is removed by prior treatment of the sample with chondroitinase ABC. ES cells derived from heterozygous mice produced ~2.3-fold less radioactive heparan sulfate than wild-type cells, suggesting that the locus is haploinsufficient. The loss of heparan sulfate is accentuated further in EXT1 −/− cells, as no heparan sulfate was detected. The loss of heparan sulfate in cells containing a null allele was accompanied by a stimulation of chondroitin sulfate formation. This effect was observed previously in CHO cell mutants altered in heparan sulfate formation (Lidholt *et al.*, 1992, Wei *et al.*, 2000).

The polymerization of heparan sulfate is generated by alternating addition of N-acetylglucosamine (GlcNAc) and glucuronic acid (GlcA) units. To confirm that the loss of heparan sulfate in the ES cells was due to deficient polymerization, we assayed the activity of the two corresponding enzyme activities in cell extracts prepared from embryoid bodies. As shown in Table 3, the decrease in heparan sulfate formation in cells correlated with loss of both GlcNAc and GlcA transferase activities *in vitro*. These findings confirm that loss of one or both EXT alleles causes a striking decrease in heparan sulfate formation. The residual enzyme activity in the −/− embryoid bodies may be due to a second mechanism for assembling heparan sulfate, possibly encoded by EXT2 or the EXT-related loci.

DISCUSSION

The abnormal development of extraembryonic tissues in EXT1-deficient embryos suggests a role for EXT1 in egg-cylinder formation. RT-PCR analysis of *in vitro* differentiated EXT1 −/− ES cells with different molecular markers demonstrated defects in mesoderm and endoderm differentiation. The expression patterns of BMP2 and BMP4, two markers for extraembryonic mesoderm, are also abnormal. In *Drosophila* mutants that lack *tout-velu*, Hedgehog proteins can signal only at a lower efficiency and to cells immediately adjacent to Hh-producing cells, while in *tout-velu*-positive cells, Hedgehog can signal to cells many cell diameters away (Bellaiche *et al.*, 1998). This defect is due to a failure in the production of heparan sulfate to which Hedgehog binds and uses as part of its diffusion mechanism (The *et al.*, 1999). EXT1 seems to function as a part of a complex encoding glycosyltransferase activities involved in

TABLE 3

Deficient Heparan Sulfate Copolymerizing Activities in Mutant and Wild-Type ES Cells

Cell line	GlcNAc transferase (pmol/min/mg)	GlcA transferase (pmol/min/mg)
+/+	91 ± 0.2	113 ± 3
+/−	22 ± 5	29 ± 3
−/−	7 ± 0.4	7 ± 0.6

Note. GlcNAc and GlcA transferase activities were measured in cell extracts (see Materials and Methods). The indicated values reflect the average of duplicate determinations ± the range.

the polymerization of heparan sulfate (Lind *et al.*, 1998; McCormick *et al.*, 1998, 2000; Wei *et al.*, 2000). Cell surface GAGs have been implicated in the binding of many types of signaling molecules. In particular heparan sulfate GAGs have been documented to mediate FGF sequestration, stabilization, and high-affinity receptor binding and signaling (as reviewed by Vlodavsky *et al.*, 1996). Our data indicate that the Ihh-N association/targeting to the cell membrane compartment may be affected by the presence of EXT1-synthesized glycosaminoglycans even in Hedgehog-producing cells. This effect becomes even more crucial to cells not adjacent to the Hedgehog-producing cells where local Ihh-N concentration is low. This is consistent with the observation that EXT1 is required for Hedgehog diffusion and/or signaling in mammals.

At E6.5, EXT1 is strongly expressed in the epiblast where the primitive streak is formed and gastrulation is initiated. Embryos that lack EXT1 fail to undergo normal gastrulation and fail to develop mesoderm. Abnormal extraembryonic tissue formation and gastrulation defects have also been reported in a number of other mutant embryos, including Smad2 and Smad4 (Weinstein *et al.*, 1998; Sirard *et al.*, 1998; Yang *et al.*, 1998), important components of the signaling pathway of the TGF-β-related factors (Lagna *et al.*, 1996). Mice lacking either the type I bone morphogenetic protein receptor or the type I activin receptor, ActRIB, also fail to make normal extraembryonic membranes or mesoderm (Mishina *et al.*, 1995; Gu *et al.*, 1998). It has been shown that the *tout-velu* mutation does not affect signaling pathways outside the Hedgehog pathway (The *et al.*, 1999). However, it is possible that the situation in mammals is more complex. It is likely that the integrated actions of several signaling pathways are responsible for the early embryonic phenotype of EXT1 knockout mice.

Human EXT patients develop multiple benign bone tumors and generally have short stature. During normal bone development, the chondrocytes are thought to be maintained in a state competent to undergo proliferation by Ihh, through the upregulation of parathyroid hormone-related protein (PTHrP) expression at the tip of the growth plate (Vortkamp *et al.*, 1996; Karp *et al.*, 2000). To effectively signal to the PTHrP-expressing cells, the diffusion of Ihh is vital. Defects in Ihh diffusion might be expected to cause reduction in bone length, resulting in the short stature seen in EXT patients. However, repression of Ihh signaling due to mutation of Ihh diffusion would be expected only to cause chondrocytes to exit proliferative states prematurely, not to induce the ectopic growth required for exostoses development. Cell–cell signaling via FGFs and their receptors (FGFRs) has been shown to be involved in coordinating the growth of endochondral and intramembranous bones (De Luca *et al.*, 1999; Muenke *et al.*, 1995). The FGFR1 and FGFR2 mutations affect intramembranous bones, while mutations in FGFR3 generally affect endochondral bones. In fact, the FGFR3-deficient mice exhibit overgrowth of the long bones (Colvin *et al.*, 1996). Since cell surface heparan sulfate is known to mediate the binding of FGFs and their FGFRs (Vlodavsky *et al.*, 1996), we hypothesize that EXT1-synthesized GAGs interact with FGFs and their receptors and affect their regulatory functions in bone development.

In humans, hereditary multiple exostosis is an autosomal dominant condition. We suggest that the short stature phenotype may be related to the haploinsufficiency of the glycosyltransferase activity as described above. Although no exostoses phenotype has been observed in EXT1 heterozygotes, a 10% loss in bone length was observed in these mice compared to wild types (data not shown). A more than 50% decline in heparan sulfate formation and ~75% decrease of GlcNAc and GlcA transferase activities were observed in EXT1 heterozygous ES cells. This further demonstrates that the haploinsufficiency of the EXT1 locus is also true for mice. The different requirement for heparan sulfate during development and the physiological difference between human and mouse may account for the minimal phenotype observed in EXT1 heterozygous mice. At least two genetic loci are responsible for EXT in human. Heterozygous mutations in either EXT1 or EXT2 locus lead to the disease phenotype in human. McCormick *et al.* (2000) demonstrated that EXT1 and EXT2 formed a heterodimer *in vivo*, which is apparently required for transit of both proteins to the Golgi apparatus. The Golgi-localized EXT1/EXT2 complex is thought to be the biological relevant form of the enzymes, since the nucleotide sugar transporters that supply the sugar precursors for heparan sulfate are localized in this compartment (Hirschberg *et al.*, 1998). This finding may explain why inherited mutations in either of the two EXT genes can cause loss of enzyme activity, resulting in exostoses. Further analyses, such as generating EXT1 chimeric mice with EXT −/− ES cell lines, EXT1/EXT2 double-heterozygous mutant mice, and tissue-specific conditional alleles of EXT1 and EXT2 will likely provide tools to study the correlation of EXT genes and bone development.

ACKNOWLEDGMENTS

We thank Qiuxia Guo and Pei Wang for expert technical assistance, Drs. William Klein and Lin Gan for pLGII vector and helpful comments about this work, Dr. Richard Behringer for the Brachyury probe, and Dr. Scott Selleck for his invaluable discussions and support. This work was supported by NIH Grant HD27981 to D.E.W. and NIH Grants GM 33063 and PPG HL57345 to J.D.E.

REFERENCES

Ahn, J., Ludecke, H. J., Lindow, S., Horton, W. A., Lee, B., Wagner, M. J., Horsthemke, B., and Wells, D. E. (1995). Cloning of the putative tumour suppressor gene for hereditary multiple exostoses (EXT1). *Nat. Genet.* **11,** 137–143.

Bame, K. J., and Esko, J. D. (1989). Undersulfated heparan sulfate in a Chinese hamster ovary cell mutant defective in heparan sulfate *N*-sulfotransferase. *J. Biol. Chem.* **264,** 8059–8065.

Becker, S., Wang, Z. J., Massey, H., Arauz, A., Labosky, P., Hammerschmidt, M., St-Jacques, B., Bumcrot, D., McMahon, A., and Grabel, L. (1997). A role for Indian hedgehog in extraembryonic endoderm differentiation in F9 cells and the early mouse embryo. *Dev. Biol.* **187,** 298–310.

Bellaiche, Y., The, I., and Perrimon, N. (1998). Tout-velu is a *Drosophila* homologue of the putative tumour suppressor EXT-1 and is needed for Hh diffusion. *Nature* **394,** 85–88.

Bitgood, M. J., and McMahon, A. P. (1995). Hedgehog and BMP genes are coexpressed at many diverse sites of cell–cell interaction in the mouse embryo. *Dev. Biol.* **172,** 126–138.

Bueno, D., Skinner, J., and Abud, H., and Heath, J. K. (1996). Spatial and temporal relationships between Shh, Fgf4, and Fgf8 gene expression at diverse signalling centers during mouse development. *Dev. Dyn.* **207,** 291–299.

Colvin, J. S., Bohne, B. A., Harding, G. W., McEwen, D. G., and Ornitz, D. W. (1996). Skeletal overgrowth and deafness in mice lacking fibroblast growth factor receptor 3. *Nat. Genet.* **12,** 390–397.

De Luca, F., and Baron, J. (1999). Control of bone growth by fibroblast growth factors. *Trends Endocrinol. Metab.* **10,** 61–65.

Doetschman, T. C., Eistetter, H., Katz, M., Schmidt, W., and Kemler, R. (1985). The in vitro development of blastocyst-derived embryonic stem cell lines: Formation of visceral yolk sac, blood islands and myocardium. *J. Embryol. Exp. Morphol.* **87,** 27–45.

Dziadek, M. (1979). Cell differentiation in isolated inner cell masses of mouse blastocysts *in vitro:* Onset of specific gene expression. *J. Embryol. Exp. Morphol.* **53,** 367–379.

Elefanty, A. G., Robb, L., Birner, R., and Begley, C. G. (1997). Hematopoietic-specific genes are not induced during in vitro differentiation of scl-null embryonic stem cells. *Blood* **90,** 1435–1447.

Ericson, J., Morton, S., Kawakami, A., Roelink, H., and Jessell, T. M. (1996). Two critical periods of Sonic hedgehog signaling required for the specification of motor neuron identity. *Cell* **87,** 661–673.

Esko, J. D., Elgavish, A., Prasthofer, T., Taylor, W. H., and Weinke, J. L. (1986). Sulfate transport-deficient mutants of Chinese hamster ovary cells: Sulfation of glycosaminoglycans dependent on cysteine. *J. Biol. Chem.* **261,** 15725–15733.

Evans, M. J., and Kaufman, M. H. (1981). Establishment in culture of plutipotential cells from mouse embryos. *Nature* **292,** 154–156.

Grabel, L., Becker, S., Lock, L., Maye, P., and Zanders, T. (1998). Using EC and ES cell culture to study early development: Recent observations on Indian hedgehog and Bmps. *Int. J. Dev. Biol.* **42,** 917–925.

Gu, Z., Nomura, M., Simpso, B. B., Lei, H., Feijen, A., van den Eijnden-van Raaij, J., Donahoe, P. K., and Li, E. (1998). The type I activin receptor ActRIB is required for egg cylinder organization and gastrulation in the mouse. *Genes Dev.* **12,** 844–857.

Hecht, J. T., Hogue, D., Strong, L. C., Hansen, M. F., Blanton, S. H., and Wagner, M. (1995). Hereditary multiple exostosis and chondrosarcoma: Linkage to chromosome 11 and loss of heterozygosity for EXT-linked markers on chromosomes 11 and 8. *Am. J. Hum. Genet.* **56,** 1125–1131.

Herrmann, B. G. (1991). Expression pattern of the Brachyury gene in whole-mount TWis/TWis mutant embryos. *Development* **113,** 913–917.

Hirschberg, C. B., Robbins, P. W., and Abeijon, C. (1998). Transporters of nucleotide sugars, ATP, and nucleotide sulfate in the endoplasmic reticulum and Golgi apparatus. *Annu. Rev. Biochem.* **67,** 49–69.

Karp, S. J., Schipani, E., St-Jacques, B., Hunzelman, J., Kronenberg, H., and McMahon, A. P. (2000). Indian hedgehog signaling regulates proliferation and differentiation of chondrocytes and is essential for bone formation. *Genes Dev.* **13,** 2072–2086.

Keller, G., Kennedy, M., Papayannopoulou, T., and Wiles, M. V. (1993). Hematopoietic commitment during embryonic stem cell differentiation in culture. *Mol. Cell Biol.* **13,** 473–478.

Kispert, A., and Hermann, B. G. (1993). The Brachyury gene encodes a novel DNA binding protein. *EMBO J.* **12,** 4898–4899.

Lagna, G., Hata, A., Hemmati-Brivanlou, A., and Massague, J. (1996). Partnership between DPC4 and SMAD proteins in TGF-beta signalling pathways. *Nature* **383,** 832–836.

Laufer, E., Nelson, C. E., Johnson, R. L., Morgan, B. A., and Tabin, C. (1994). Sonic hedgehog and Fgf-4 act through a signaling cascade and feedback loop to integrate growth and patterning of the developing limb bud. *Cell* **79,** 993–1003.

Lee, J. J., von Kessler, D. P., Parks, S., and Beachy, P. A. (1992). Secretion and localized transcription suggest a role in positional signaling for products of the segmentation gene hedgehog. *Cell* **71,** 33–50.

Lee, J. J., Ekker, S. C., von Kessler, D. P., Porter, J. A., Sun, B. I., and Beachy, P. A. (1994). Autoproteolysis in hedgehog protein biogenesis. *Science* **266,** 1528–1537.

Lidholt, K., Weinke, J. L., Kiser, C. S., Lugemwa, F. N., Bame, K. J., Cheifetz, S., Massagué, J., Lindahl, U., and Esko, J. D. (1992). A single mutation affects both *N*-acetylglucosaminyltransferase and glucuronosyltransferase activities in a Chinese hamster ovary cell mutant defective in heparan sulfate biosynthesis. *Proc. Natl. Acad. Sci. USA* **89,** 2267–2271.

Lin, X., and Wells, D. (1997). Isolation of the mouse cDNA homologous to the human EXT1 gene responsible for hereditary multiple exostoses. *DNA Seq.* **7,** 199–202.

Lin, X., Gan, L., Klein, W. H., and Wells, D. (1998). Expression and functional analysis of mouse EXT1, a homolog of the human multiple exostoses type 1 gene. *Biochem. Biophys. Res. Commun.* **248,** 738–743.

Lind, T., Tufaro, F., McCormick, C., Lindahl, U., and Lidholt, K. (1998). The putative tumor suppressors EXT1 and EXT2 are glycosyltransferases required for the biosynthesis of heparan sulfate. *J. Biol. Chem.* **273,** 26265–26268.

Matzuk, M. M., Finegold, M. J., Su, J. G., Hsueh, A. J., and Bradley, A. (1992). Alpha-inhibin is a tumour-suppressor gene with gonadal specificity in mice. *Nature* **360,** 313–319.

McCormick, C., Leduc, Y., Martindale, D., Mattison, K., Esford, L. E., Dyer, A. P., and Tufaro, F. (1998). The putative tumour suppressor EXT1 alters the expression of cell-surface heparan sulfate. *Nat. Genet.* **19,** 158–161.

McCormick, C., Duncan, G., Goutsos, K. T., and Tufaro, F. (2000). The putative tumor suppressors EXT1 and EXT2 form a stable complex that accumulates in the Golgi apparatus and catalyzes the synthesis of heparan sulfate. *Proc. Natl. Acad. Sci. USA* **297,** 668–673.

Mishina, Y., Suzuki, A., Ueno, N., and Behringer, R. R. (1995). Bmpr encodes a type I bone morphogenetic protein receptor that is essential for gastrulation during mouse embryogenesis. *Genes Dev.* **9,** 3027–3037.

Muenke, M., and Schell, U. (1995). Fibroblast-growth-factor receptor mutations in human skeletal disorders. *Trends Genet.* **11,** 308–313.

Poirier, F., Chan, C. T., Timmons, P. M., Robertson, E. J., Evans, M. J., and Rigby, P. W. (1991). The murine H19 gene is activated during embryonic stem cell differentiation in vitro and at the time of implantation in the developing embryo. *Development* **113,** 1105–1114.

Porter, J. A. (1995). The product of hedgehog autoproteolytic cleavage active in local and long-range signalling. *Nature* **374,** 363–366.

Roach, S., Schmid, W., and Pera, M. F. (1994). Hepatocytic transcription factor expression in human embryonal carcinoma and yolk sac carcinoma cell lines: Expression of HNF-3α in models of early endodermal cell differentiation. *Exp. Cell Res.* **215,** 189–198.

Roberts, D. J., Johnson, R. L., Burke, A. C., Nelson, C. E., Morgan, B. A., and Tabin, C. (1995). Sonic hedgehog is an endodermal signal inducing Bmp-4 and Hox genes during induction and regionalization of the chick hind gut. *Development* **121,** 3163–3174.

Robertson, E. J. (1987). Embryo-derived stem cell lines. *In* "Teratocarcinoma and Embryonic Stem Cells: A Practical Approach" (E. J. Robertson, Ed.), pp. 71–112. IRL Press, Oxford.

Sirard, C., de la Pompa, J. L., Elia, A., Itie, A., Mirtsos, C., Cheung, A., Hahn, S., Wakeham, A., Schwartz, L., Kern, S. E., Rossant, J., and Mak, T. W. (1998). The tumor suppressor gene Smad4/Dpc4 is required for gastrulation and later for anterior development of the mouse embryo. *Genes Dev.* **12,** 107–119.

Soudais, C., Bielinska, M., Heikinheimo, M., MacArthur, C. A., Narita, N., Saffitz, J. E., Simon, M. C., Leiden, J. M., and Wilson, D. B. (1995). Targeted mutagenesis of the transcription factor GATA-4 gene in mouse embryonic stem cells disrupts visceral endoderm differentiation in vitro. *Development* **121,** 3877–3888.

Stickens, D., Clines, G., Burbee, D., Ramos, P., Thomas, S., Hogue, D., Hecht, J. T., Lovett, M., and Evans, G. A. (1996). The EXT2 multiple exostoses gene defines a family of putative tumour suppressor genes. *Nat. Genet.* **14,** 25–32.

St-Jacques, B., Hammerschmidt, M., and McMahon, A. P. (1999). Indian hedgehog signaling regulates proliferation and differentiation of chondrocytes and is essential for bone formation. *Genes Dev.* **13,** 2072–2086.

The, I., Bellaiche, Y., and Perrimon, N. (1999). Hedgehog movement is regulated through tout velu-dependent synthesis of a heparan sulfate proteoglycan. *Mol. Cell* **4,** 633–639.

Toyoda, H., Kinoshita-Toyoda, A., and Selleck, S. B. (2000). Structural analysis of glycosaminoglycans in Drosophila and Caenorhabditis elegans and demonstration that tout-velu, a Drosophila gene related to EXT tumor suppressors, affects heparan sulfate in vivo. *J. Biol. Chem.* **275,** 2269–2275.

Vlodavsky, I., Miao, H. Q., Medalion, B., Danagher, P., and Ron, D. (1996). Involvement of heparan sulfate and related molecules in sequestration and growth promoting activity of fibroblast growth factor. *Cancer Metastasis Rev.* **15,** 177–186.

Vortkamp, A., Lee, K., Lanske, B., Segre, G. V., Kronenberg, H. M., and Tabin, C. J. (1996). Regulation of rate of cartilage differentiation by Indian hedgehog and PTH-related protein. *Science* **273,** 613–622.

Wei, G., Bai, X., Bame, K. J., Koshy, T. I., Spear, P. G., and Esko, J. D. (2000). Expression cloning of heparan sulfate copolymerase (EXT1) and analysis of mutations in Chinese hamster ovary cell mutants defective in heparan sulfate biosynthesis. Submitted for publication.

Weinstein, M., Yang, X., Li, C. L., Xu, X. L., Gotay, J., and Deng, C. X. (1998). Failure of egg cylinder elongation and mesoderm induction in mouse embryos lacking the tumor suppressor Smad2. *Proc. Natl. Acad. USA* **95,** 9378–9383.

Wicklund, C. L., Pauli, R. M., Johnston, D., and Hecht, J. T. (1995). Natural history study of hereditary multiple exostoses. *Am. J. Med. Genet.* **55,** 43–46.

Wilkinson, D. G., and Nieto, M. A. (1993). Detection of messenger RNA by in situ hybridization to tissue sections and whole mounts. *Methods Enzymol.* **225,** 361–373.

Winnier, G., Blessing, M., Labosky, P. A., and Hogan, B. L. (1995). Bone morphogenetic protein-4 is required for mesoderm formation and patterning in the mouse. *Genes Dev.* **9,** 2105–2116.

Yang, X., Li, C. L., Xu, X. L., and Deng, C. X. (1998). The tumor suppressor SMAD4/DPC4 is essential for epiblast proliferation and mesoderm induction in mice. *Proc. Natl. Acad. Sci. USA* **95,** 3667–3672.

Zhang, H., and Bradley, A. (1996). Mice deficient for BMP2 are nonviable and have defects in amnion/chorion and cardiac development. *Development* **122,** 2977–2986.

Zou, H., Wieser, R., Massague, J., and Niswander, L. (1997). Distinct roles of type I bone morphogenetic protein receptors in the formation and differentiation of cartilage. *Genes Dev.* **11,** 2191–2203.

Received for publication March 23, 2000
Revised May 30, 2000
Accepted May 26, 2000